

Physical modelling of soil liquefaction in a novel micro shaking table

Fausto Molina-Gómez^{*1}, Bernardo Caicedo^{2a} and António Viana da Fonseca^{1b}

¹Faculty of Engineering (FEUP), CONSTRUCT-GEO, Universidade do Porto, Porto, Portugal

²Department of Civil and Environment Engineering, Universidad de Los Andes, Bogotá, Colombia

(Received July 16, 2018, Revised October 8, 2019, Accepted October 15, 2019)

Abstract. The physical models are useful to understand the soil behaviour. Hence, these tools allow validating analytical theories and numerical data. This paper addresses the design, construction and implementation of a physical model able to simulate the soil liquefaction under different cyclic actions. The model was instrumented with a piezoelectric actuator and a set of transducers to measure the porewater pressures, displacements and accelerations of the system. The soil liquefaction was assessed in three different grain size particles of a natural sand by applying a sinusoidal signal, which incorporated three amplitudes and the fundamental frequencies of three different earthquakes occurred in Colombia. In addition, such frequencies were scaled in a micro shaking table device for 1, 50 and 80 g. Tests allowed identifying the liquefaction susceptibility at various frequency and displacement amplitude combinations. Experimental evidence validated that the liquefaction susceptibility is higher in the fine-grained sands than coarse-grained sands, and showed that the acceleration of the actuator controls the phenomena triggering in the model instead of the displacement amplitude.

Keywords: Guamo sand; pore-water pressure excess; soil liquefaction; soil modelling

1. Introduction

Earthquakes are one of the greatest hazards to infrastructure and human life. After to Alaska and Niigata earthquakes, the liquefaction phenomenon has been widely studied in geotechnical engineering since liquefaction is one of the most devastating instabilities in saturated granular materials (Ramos *et al.* 2015). This phenomena occurs when the effective stress of the soil is zero and is associated with the stiffness reduction (Idriss and Boulanger 2008). Loose clean sands are more susceptible to trigger liquefaction because this kind of soil tends to compact under cyclic or monotonic undrained loading. The critical state soil mechanics (CSSM) framework explains the contractile/dilative behaviour of the sands through the state parameter, ψ , (Been and Jefferies 1985). During the loading, the soil volume tends to decrease causing an increment of pore water pressure, which cannot dissipate under undrained conditions. This phenomenon may trigger under static conditions (e.g., seepage, water level rise or rapid overloading) or cyclic conditions (e.g., earthquakes, machine vibration or traffic action). Usually, the soil liquefaction is identified when the pore pressure increment (ΔU) is equal to the initial mean effective stress (p'). The ratio between ΔU and p' represents the pore pressure excess parameter (r_u).

Several field techniques and laboratory methods have been developed to assess the liquefaction resistance. Seed and Idriss (1971) suggested a methodology to estimate the safety factor of liquefaction from SPT results. Such methodology is easy to apply and widely used to evaluate the liquefaction resistance. Robertson and Wride (2010), and Robertson (2010) established procedures to estimate the cyclic and flow liquefaction susceptibility, respectively, by CPTu tests. These procedures are an approach for evaluating the dilative or contractile behaviour using the state parameter, ψ . Alarcón-Guzmán *et al.* (1988) presented results of the monotonic and cyclic tests, which describe the soil behaviour during pore water pressure built-up. These authors proposed the quasi steady state (QSS) for identifying the changes from contractile to dilative behaviour in sandy soils. Georgiannou *et al.* (2008) evaluated the liquefaction susceptibility, stiffness and damping characteristics of the Fontainebleau sand using torsional tests. These authors identified tendency to dilation after the QSS or the phase of volumetric transformation in hollow specimens. Viana da Fonseca *et al.* (2015) performed an experimental plan in different sands including cyclic direct simple shear to establish the effect of relative density in the liquefaction susceptibility. These authors compared their results with triaxial tests done in the same soils. Monkul *et al.* (2015) conducted a series of cyclic simple shear tests responses in clean and silty sands to identify the fine contents effect in soil liquefaction. These authors validated that the liquefaction resistance in dry and saturated specimens increases with the fine contents of the soil.

However, the field and laboratory tests must be complemented to estimate the liquefaction susceptibility. An excellent alternative to complement these tests is the physical modelling. Physical modelling can be performed in centrifuge or shaking table equipments. Hushmand *et al.*

*Corresponding author, M.Sc.

E-mail: fausto@fe.up.pt

^aProfessor

E-mail: viana@fe.up.pt

^bProfessor

E-mail: bcaicedo@uniandes.edu.co

(1988) implemented a device to assess the soil response of dry and saturated sands under earthquake excitations. Such device included a box constructed of aluminium laminae designed to move freely on each other. Madabhushi and Schofield (1993) conducted a series of tests in geotechnical centrifuge applying the scaled fundamental frequency of two different earthquakes. Their results indicated that the soil experiments a stiffness degradation during the liquefaction phenomena due to the increment of pore water pressure in the models. Cohelo *et al.* (2006) presented a series of centrifuge test intended to enhance the understanding of the effects of successive strong earthquakes on uniform saturated sand deposits. These authors found that strain amplitudes of the seismic simulations are independent of the magnitude of the seismic energy transmitted to the deposit of soil during liquefaction triggering. Turan *et al.* (2009) designed a laminar box to evaluate the soil-structure interaction in a shaking table device. Their results showed that the laminar box does not impose significant boundary effects and is able to maintain 1-D soil column behaviour. Dashti *et al.* (2010) performed three centrifuge experiments to generate well-documented model “case histories” of building response on liquefied ground. The centrifuge tests provided information about the relative importance of the thickness and density of the liquefiable soil layer, as well as the effects of various foundation characteristics on building performance. Ueng *et al.* (2010) performed tests on a shaking table to measure the volumetric strains of a clean sand during sinusoidal cyclic loading. They establish that the settlement of the models, during shaking, is small and significant volume changes occur only after the sand liquefies. Wang *et al.* (2011) evaluated the influence of the dissipation of pore pressure excess on liquefaction-induced ground deformation using shaking table tests. Their experimental plan included the preparation of 1 g physical models with Toyura sand, where the viscosity of the soil-saturation fluid was changed in order to estimate the effect of soil permeability in the settlement and lateral displacement of the soil. Bertalot and Brennan (2015) performed geotechnical centrifuge test to present the apparently counter-intuitive relationship between settlement and footing bearing stress. Their results clarified the hypothesis that although increasing the bearing pressure of shallow foundations on liquefiable soil causes an increase in likely settlement. Zhou *et al.* (2015) combined the centrifuge and shaking table devices to study the micro-behaviour of saturated sand around a buried structure. They found that the pore pressure ratio was generally higher for sand around the structure and it increased more significantly at the bottom than on the sides of the structure, which was due to the change of dissipation pattern of excess pore pressure by the buried structure.

This work aims to present the design of a flexible container and its implementation in a micro shaking device to evaluate the soil liquefaction due to cyclic loads. Besides, the document discusses the mechanism to trigger the liquefaction using three different scaling factors for models at 1 g. Such scaling factors were selected to evaluate the behaviour in shallow deposits of liquefiable soils for different input signals. The document structure is as follows. The first section corresponds to the introduction and the literature review of this research. The second section presents a theoretical background concerning the

physical modelling of soil liquefaction. The third section describes the studied soil, the model instrumentation and the experimental plan. The fourth section covers the analysis of the results. The fifth section discusses the findings and shows the liquefaction resistance curves obtained from the physical models. Finally, the sixth section presents the conclusions of this research.

2. Liquefaction physical modelling

The geotechnical engineers have made many investigations and analysis to identify the causes (soil behaviour) and the effects (infrastructure damage) of liquefaction phenomena. The main advances have been developed in the laboratory. However, the implementation of field procedures is necessary to fully understand the phenomena. In addition, the field tests required an experimental camp with all the conditions to assess the phenomena. Within these conditions are included a widespread area, a mechanism to apply the earthquake and a set of transducers to measure the soil response. Therefore, the constructions of scale models are used to represent the initial conditions of liquefaction. For earthquake engineering purposes, scale models are usually well instrumented and then tested using shaking tables or centrifuge devices (Kramer and Elgamal 2001). In complex projects, a comparison between centrifuge tests with finite elements is the best option to validate both results.

2.1 Centrifuge modelling (Ng)

According to engineering design, it is usual to evaluate geotechnical structures by the construction of scaled models. These models can be build and, after, tested in centrifuge equipment to represents the soil behaviour of the prototype. Modelling of geotechnical problems in the centrifuge aims to test a reduced-scale model 1/N generating an acceleration field that is N times Earth’s gravity (Caicedo *et al.* 2015). When the centrifuge model subjected to an inertial acceleration field of N times Earth’s gravity, the vertical stress at depth (h_m) will be identical to that in the corresponding prototype at depth (h_p), as Eq (1) shows

$$h_p = N \cdot h_m \quad (1)$$

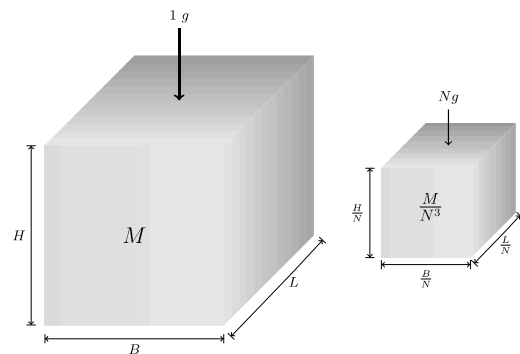


Fig. 1 Principle of centrifuge modelling. Adapted from Madabhushi (2014)

Table 1 Scaling factors for centrifuge modelling (Taylor, 1995)

Type of event	Parameter	Scaling law <i>model/prototype</i>	Units
All events	Stress	1	N/m
	Strain	1	-
	Length	1/N	m
	Time	N	s
Diffuse events	Time (consolidation)	1/N ²	s
Dynamic events	Frequency	N	s ⁻¹
	Velocity	1	m/s ¹
	Acceleration	N	m/s ²
	Displacement	1/N	m

Table 2 Similitude factors for shaking table modelling (Iai 1989)

Parameter	Scaling law <i>model/prototype</i>	Units
Length	1/Λ	m
Strain	1	-
Stress	1	Nm ⁻²
Acceleration	1	ms ⁻²
Time	1/Λ ^{1/2}	s
Frequency	Λ ^{1/2}	s ⁻¹

To obtain a better representation, the centrifuge model must be constructed with the same soil of the prototype. The gravity is increased by the same geometric factor N relative to the normal Earth's gravity field, which is 1g Madabushi (2014). Fig. 1 describes the scale factor in centrifuge modelling.

In principle, the change of Earth's gravity produces an increment of the soil stress state. This increment affects the behaviour of the model. Therefore, the centrifuge test results of such model are compared with prototype response by the application of the scaling factors (Table 1).

2.2 Shaking table modelling (1 g)

The shaking table is another kind of apparatus for evaluating the soil behaviour through the construction of physical models. This equipment offers the advantage to testing larger soil models Kramer and Elgamal (2001). The tests performed with such devices are conducted at 1g gravitational field. At present many laboratories, which study damages of earthquakes, have shaking tables capable to produce displacements in 1, 2 or 3 dimensions. The movements in the device are generated by programmable actuators. Such actuators can be mechanical, hydraulic, pneumatic, electromagnetic or piezo-electric according to the magnitude of the stresses or displacements required to simulate the phenomenon of interest.

To simulate the prototype in the model test, the law of similitude must be applied. Initially, the similitude factor (Λ) was defined by Iai (1989). Such scaling factor was validated by Meymand (1998) using a model to simulate the seismic behaviour of piles in a saturated clay. Lin and Wang

(2006) presented the mathematical procedure that validates the computation of the similitude factors for 1g model testing. Table 2 presents the similitude factors, Λ to compare model and prototype with the same weight density at 1g in shaking table.

3. Materials and methods

3.1 Equipment

At the physical models' laboratory of the Universidad de los Andes, Serrato (2012) and Correa (2015) designed and built a laminae container to evaluate the dynamic soil behaviour on 1g and N g tests. Nevertheless, this laminar box model presented some friction between the laminae and the vertical supports, which increased and induced a non-



Fig. 2 Flexible container

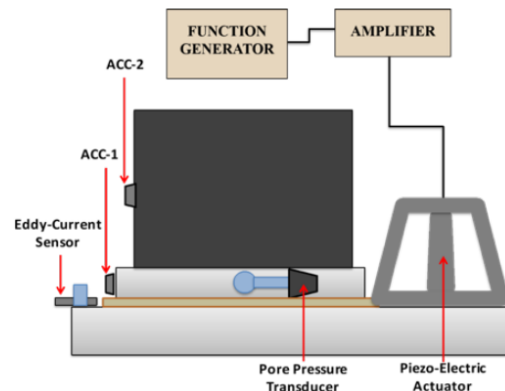


Fig. 3 Schematic view of the micro shaking table instrumentation

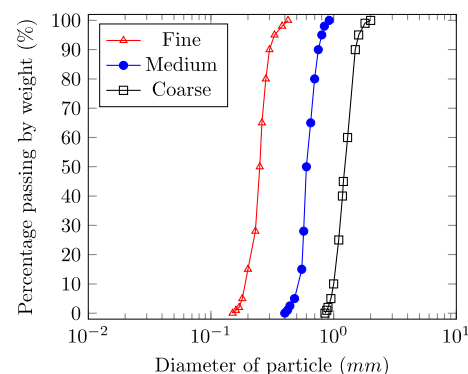


Fig. 4 Curves of grain size distribution

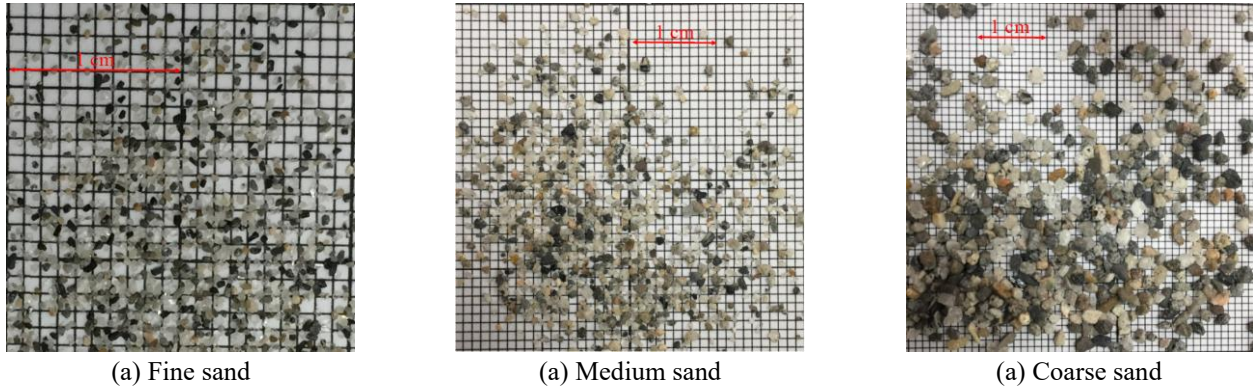


Fig. 5 Aspect of the sand grains

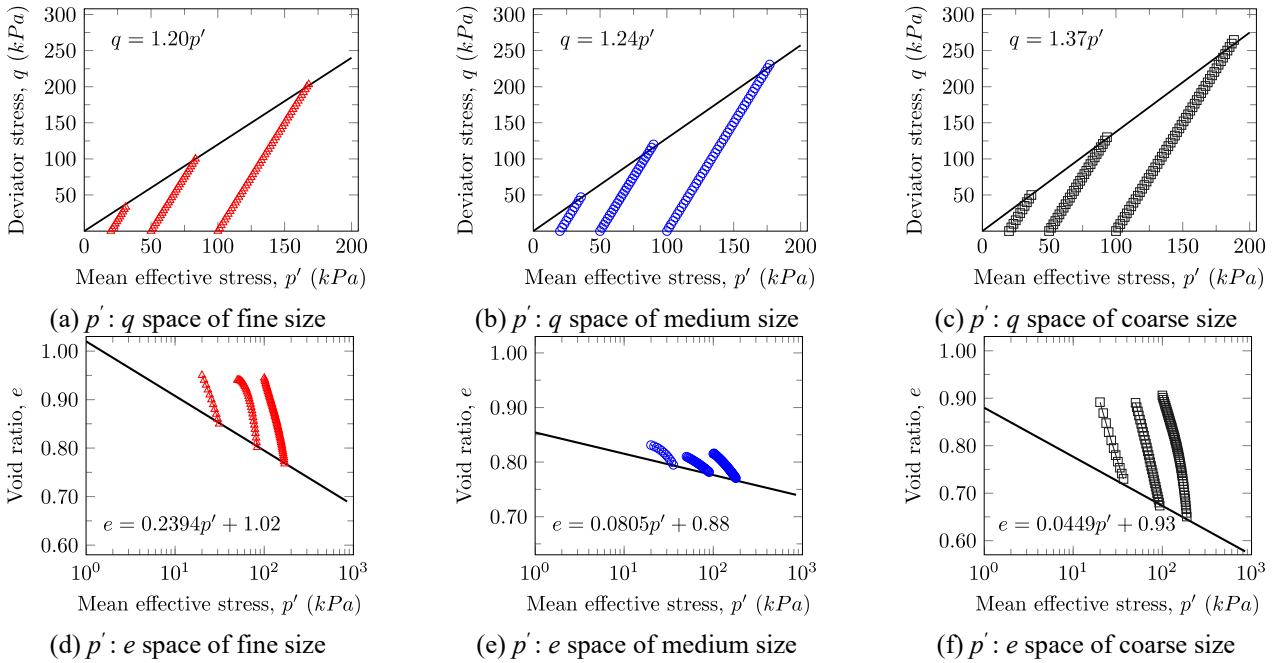


Fig. 6 Critical state of Guamo sands

Table 3 Physical properties of the Guamo sands

Parameter	Unit	Fine size	Medium size	Coarse size
G_s	-	2.70	2.66	2.67
e_{max}	-	0.99	0.84	0.96
e_{min}	-	0.65	0.67	0.56
γ_{max}	kN/m^3	15.13	15.35	14.16
γ_{min}	kN/m^3	13.31	14.18	13.36
D_{50}	mm	0.25	0.60	1.25
C_u	-	1.37	1.24	1.32

Table 4 Critical state parameters of the Guamo sands

Parameter	Unit	Fine sand	Medium sand	Coarse sand
ϕ'_{cv}	$^\circ$	30	32	34
M	-	1.20	1.29	1.37
Γ	-	1.02	0.88	0.93
λ	-	0.1041	0.0350	0.0195

representative performance at low frequencies. Therefore, a new container was built. The new flexible container was fabricated with black silicone and dimensions of 80 mm x 60 mm x 60 mm (Figure 2). This design is completely frictionless since the container walls are not in contact with other elements, such as vertical supports. Besides, it has the advantage to allow the free movement of the soil inside the box because the low stiffness of the silicone. In addition, the recipient material ensures that at the junctions no water leaks occur. Moreover, the box has a hole of 10 mm diameter in the bottom covered with a mesh of 0.075 mm (sieve 200) allowing the measurement of pore water pressure.

The flexible container was incorporated into a Micro Shaking Table able to generate dynamic loads in 1D. The system movement was applied by a Piezo-Electric actuator (CEDRAT APA ML120), which received input signal produced in a function generator (PROTEK B8003FD) and was amplified by an amplifier device (CEDRAT LA75). Besides, this Micro Shaking Table was instrumented with a sensor type Eddy-Current 0.025 μm precision (eddy-NCDDT 3010) to measure the displacements at the container bottom. Likewise, two accelerometers (ACC104A OMEGA) were positioned in the base and middle of the flexible container to register the soil response during the dynamic tests. On the other hand, a pressure transducer (Honey Well 40PC0156) was connected directly to the box bottom to measures the pore-water pressure increment of the soil when applying dynamic loading. The test data was acquired through a NI 9234 National Instruments card and Lab VIEW® code. Fig. 3 shows the system and its instrumentation.

3.2 Materials

Fine, medium and coarse particle size distributions of Guamo Sand were selected. Such selection involved the sieving process described in the standard procedure ASTM D422 and allowed obtaining parallel distribution curves. The soil selection sought to estimate the particle size effect on the liquefaction resistance. Fig. 4 displays the grain size distributions of the sands.

Geologically, the Guamo Sand is a product of the sequence of volcanic deposits coming to Machín volcano and is transported through Luisa River, which is located at Tolima department in Colombia. Mineralogically, the Guamo sand is composed by quartz in a 99% (Sarmiento and Vidal 2007). In addition, the particle shape of this of sand is predominantly sub-angular. Fig. 5 shows the shape of the grain size distribution of the Guamo Sands.

Table 3 presents the physical properties results. Specific gravity (G_s) of solid particles was estimated through the method of the standard ASTM D854. The maximum void ratio (e_{max}) of the particles sizes were evaluated based on the procedure of the INV-E 136. The minimum void (e_{min}) ratio of the particles sizes was assessed according to method C of the standard procedure ASTM D4254. The mean diameter (D_{50}) and the coefficient of uniformity (C_u) were obtained from the grain size distributions shown in Figure 4.

On the other hand, the critical state parameters for all

Table 5 Properties and critical state parameters comparisons of the similar sandy-soils

Parameter	Unit	Fine sand	Likan	Medium sand	Ottawa	Coarse sand	Monterrey
D_{50}	mm	0.25	0.24	0.60	0.60	1.25	1.30
C_u	-	1.37	1.90	1.24	1.40	1.32	1.30
e_{max}	-	0.99	1.24	0.84	0.79	0.96	0.71
e_{min}	-	0.65	0.84	0.67	0.49	0.6	0.49
ϕ'_{cv}	°	30	34.5	32	32	34	33
M	-	1.20	1.40	1.29	1.24	1.37	1.33
Γ	-	1.02	1.36	0.88	0.74	0.93	0.93
λ	-	0.1041	0.1480	0.0350	0.0530	0.0195	0.0230

Table 6 Matrix conditions of the experimental program

Parameter	Unit	Values		
Amplitude	mV	200	500	800
Frequency ($\Lambda = 1$)	Hz	1.34	1.80	2.04
Frequency ($\Lambda = 2500$)	Hz	90	105	207.5
Frequency ($\Lambda = 6400$)	Hz	144	168	332

grain size distributions were identified. Such parameters were assessed by consolidated drained (CD) triaxial tests. The test procedure was executed in four stages: (i) sample preparation by dry pluviation method; (ii) sample saturation using cell and back pressure increments of 30 kPa, until achieving a B-value higher than 0.95; (iii) soil consolidation (20, 50 and 100 kPa); (iv) shearing at 0.0275 mm/min speed until achieve 25% of axial strain. This procedure was implemented to ensure the critical state condition of the soil on samples of 70 mm diameter and 140 mm height. Figure 6 shows the stress paths and the void ratio change during the triaxial tests.

Table 4 summarises the critical state parameters of the sands. Such parameters were compared against results obtained for Guamo Sand by Patiño (2006), Jiménez and Lizcano (2015) and Tique (2016), who conducted several triaxial tests establishing values of ϕ'_{cv} between 31° and 34°. Likewise, they found void ratios values of 0.85±0.07 at the end of the shear stage.

In addition, as a complementary characterisation analysis, the critical state parameters were compared against the results reported and compiled by Cho *et al.* (2006) for sandy soils that have the most similar grain size distribution of the materials used in this work. The criteria to match the materials were the D_{50} and C_c . The sandy soils that have the best fitting for fine, medium and coarse distribution were Likan, Ottawa and Monterrey Sand, respectively. From this approach, it was observed that the shear strength values at the critical state condition are almost equal; however, the parameters in the $p' : e$ space were different between sands, probably, due to the shape of the particles. Table 5 presents the comparison between the soils.

3.3 Excitation characteristics

Fine, medium The liquefaction susceptibility was

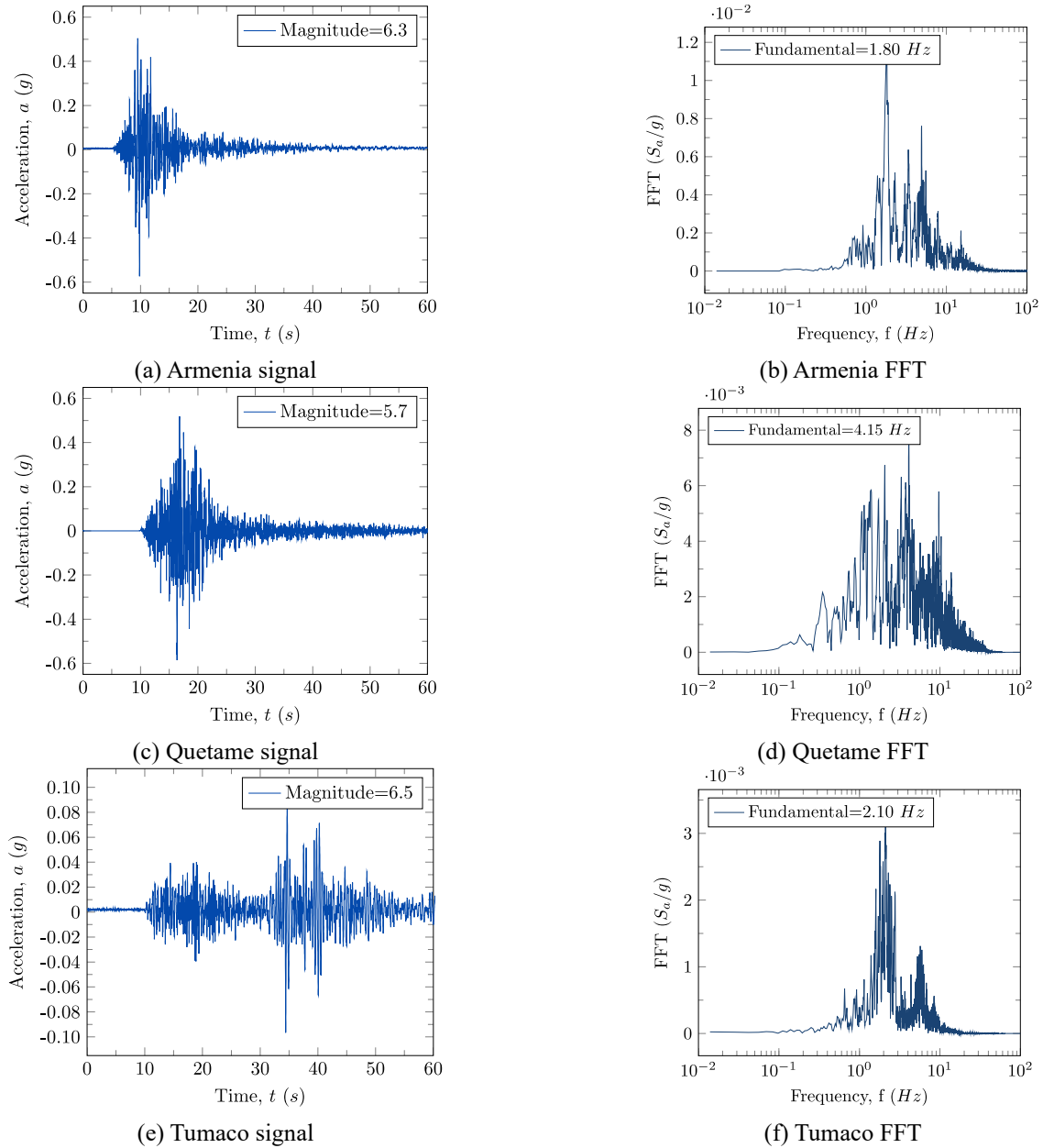


Fig. 7 Earthquake signal and spectra response

evaluated using three Colombian representative earthquakes: Armenia (1999), Quetame (2008) and Tumaco (2013). However, the function generator used in this work is limited for creating the same signals of the ground motions. Hence, the simplification of the real signals presented by Moczo *et al.* (2014) was implemented. Such simplification is based on the applying of a continuous sinusoidal signal with the fundamental frequency of the earthquake at different amplitudes. The fundamental frequency of the earthquakes signals was obtained by computing the Function Fourier Transformation (FFT). The equivalent ground motions were applied to the Micro Shaking Table equipment using the Piezo-Electric actuator. Fig. 7 presents the three earthquake signals in terms of time and frequency domains.

On the other hand, three different voltages amplified the input signal. In addition, the fundamental signals were

scaled for Λ factors of 1, 2500 and 6400 to model shallow deposits of liquefiable soils. Selected Λ allowed assessing the behaviour of Guamo Sand deposits at 0.06, 1.50 and 3.80 m depth. To estimate the liquefaction susceptibility of such deposits, an experimental program that includes 81 tests (27 for each grain size distribution of Guamo Sand) in micro shaking table was conducted. Table 6 presents the experimental program conditions.

4. Analysis of results

The implementation of the Micro Shaking Table device included a set of tests without soil. Such tests allowed assessing the displacement of the flexible container during the dynamic loading. The displacement measurements of the “Eddy-Current” sensor indicated that the system displacement is independent on the frequency of the signal.

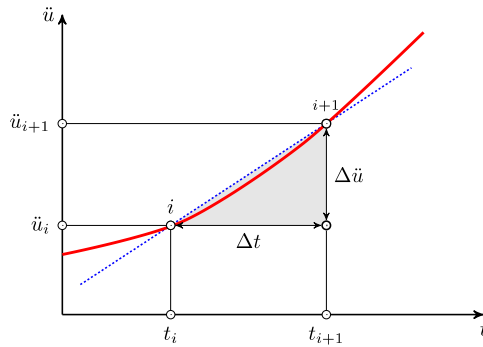


Fig. 8 Numerical integration method

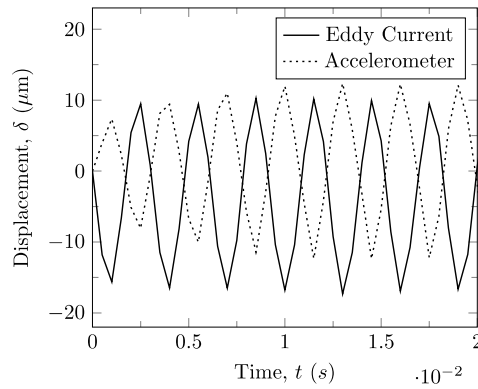


Fig. 9 Comparison of displacements, direct measurements against numerical integration

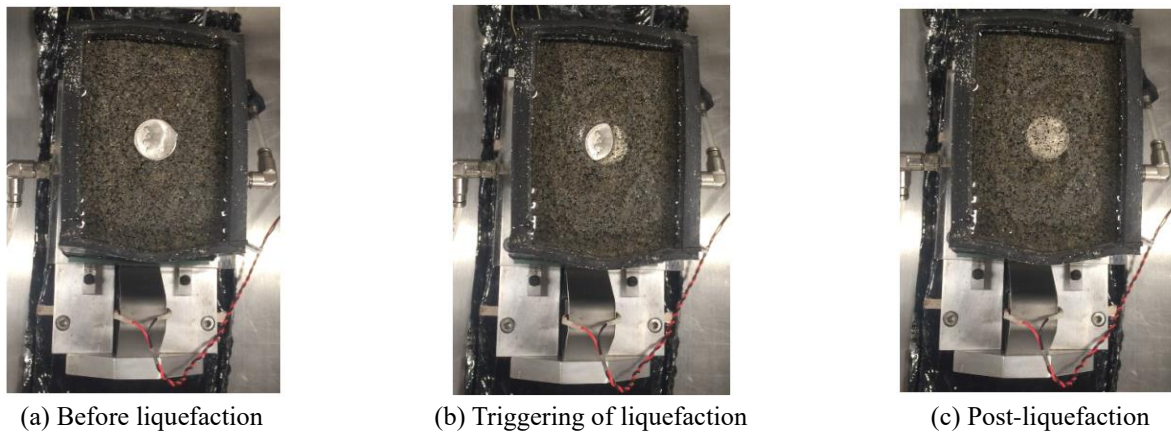


Fig. 10 Test stages

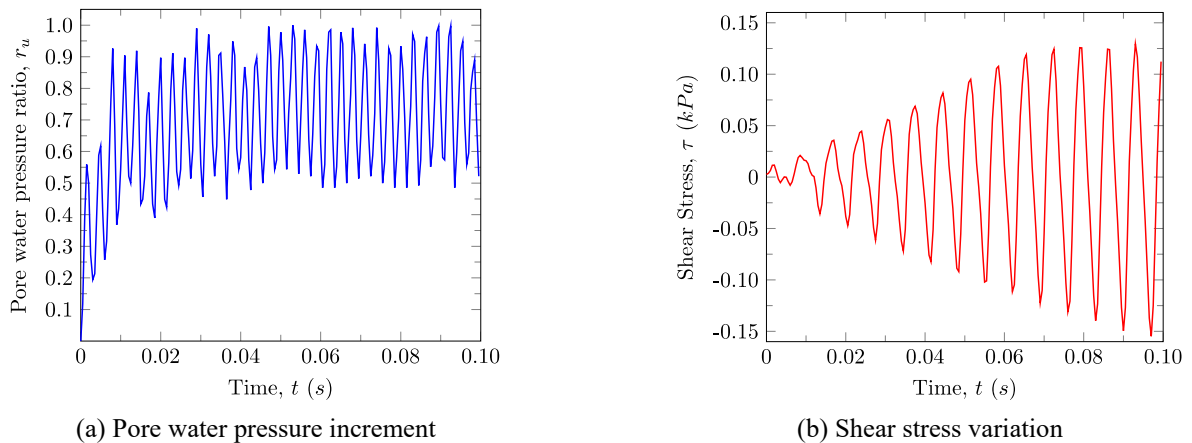


Fig. 11 Soil response

The accelerometers showed that frequency controls the system acceleration.

The test interpretation was done by association of the “Eddy-Current” sensor and accelerometers measurements. This interpretation allowed estimating the soil displacement into the flexible container. Such displacements were computed using the Duhamel’s Integral (Eq. (2)), which describes the response of a linear system, like the 1D shaking table apparatus.

$$h_p = N \cdot h_m \quad (1)$$

$$u(t) = \frac{1}{m\omega_d} \int_0^t Q(\tau) e^{-\xi\omega(t-\tau)} \sin \omega_d (t - \tau) d\tau \quad (2)$$

The Duhamel’s Integral is very difficult to solve analytically, but it can be integrated numerically (Kramer 1996). Fig. 8 presents the approximation procedure to evaluate the convolution integral by numerical methods. Since the displacement is defined as the second integral of acceleration, Eq. (3) and Eq. (4) explain the computation used to obtain the soil response by the accelerometers’ measurements in a time instant (Δt).

$$\dot{u}: \Delta \dot{u} = \ddot{u}(\tau) \Delta t + \Delta \ddot{u}(\tau) \cdot \frac{\Delta t}{2} \quad (3)$$

$$u: \Delta u = \dot{u}(\tau) \Delta t + \Delta \dot{u}(\tau) \frac{\Delta t^2}{2} + \Delta \ddot{u}(\tau) \frac{\Delta t^2}{6} \quad (4)$$

Similarly, the accelerometers’ measurements allow estimating the shear strain and shear stress of soil through the motion equations (Eq. (5) and Eq. (6)). Turan *et al.* (2009) state that the motion equation integral can be solved using the linear interpolation method between two points of the shaking table device. In this way, shear strain and shear stress values were calculated by the comparison between the readings of the accelerometers located at the middle and the basis of the flexible container.

$$\tau(z, t) = \int \rho \ddot{u} dz \quad (5)$$

$$\tau_i(t) = \sum_{k=0}^{i-1} \rho \frac{\ddot{u}_k + \ddot{u}_{k+1}}{2} \Delta Z_k \quad (6)$$

Results show that the peak to peak displacements, at the recipient base, obtained via numerical integration are close to the registered by the “Eddy-Current” sensor. Fig. 9 presents a comparison between the direct measurements of the “Eddy-Current” against the results of the numerical integration of the Duhamel’s Integral. From this comparison, it is possible to affirm that the accelerometer records can estimate displacements and stresses of the soil in the container.

Specimens of Guamo Sand were prepared by the water sedimentation method. The preparation procedure is based on three phases (Ishihara 1996): (i) water filling the container with de-aired water; (ii) soil falling from a funnel partially submerged at constant flow; and (iii) soil sedimentation during 90 minutes to allow the full saturation of the soil. This method allows obtaining homogeneous samples with lower void ratio values. Besides, the water sedimentation method guaranty the saturation of soil in physical models (Sharp *et al.* 2010).

The micro shaking table tests showed a similar soil reaction during the liquefaction process as reported in 2011 Christchurch (New Zealand) earthquake obtained by Green *et al.* (2012). Fig. 10 shows the model behaviour during the test. This Figure presents three different moments of testing: (i) the initial conditions of the soil before liquefaction; (ii) the triggering of liquefaction, in which is observed by the water rise towards the surface; and (iii) the post-liquefaction settlement due to loss of stiffness and rearrangement of particles after the dynamic action.

The triggering of liquefaction was assessed by the measurement of pore pressure increment using the pore water pressure ratio ($r_u = \Delta U / p'_0$). The samples that registered values of $r_u > 0.90$ were considered as liquefied (Du and Chian 2018). For all tests the number of cycles to achieve the liquefaction criterion were registered and the pore pressure. In addition, the pore water ratio and the variation of the shear stress were plotted against in function the time, in order to confirm the liquefaction occurrence via the sudden decreasing of soil stiffness. Fig. 11 shows the soil response during the dynamic loading application.

Results show that the frequency of the input signal controls the trigger of liquefaction phenomena in micro shaking table tests. Since the high frequencies generate high accelerations in the system and, simultaneously, such accelerations induce the pore pressure build-up. When applying of dynamic loading under high frequencies, the soil cannot dissipate the excess of pore water pressure in free field. Therefore, tests performed at frequencies lower than 105 Hz do not trigger the liquefaction phenomena. Table 6 presents the initial state of the soil and indicates the triggering liquefaction for each sample.

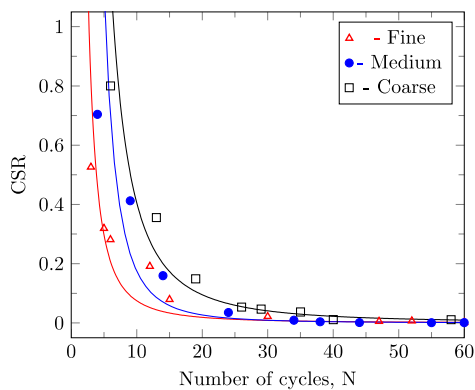
5. Discussion

During the experimental plan, 81 physical models in the micro shaking table were prepared and tested to evaluate the susceptibility of soil liquefaction phenomena in three different grain size distributions of Guamo Sand. Only 33 tests triggered liquefaction, 12 in fine sand, 11 in the medium sand and 10 in coarse sand. The cycles to trigger the phenomena were estimated and plotted against the cyclic stress ratio (CSR). As before-mentioned, the number of cycles to consider the triggering of soil liquefaction were registered when $r_u > 0.90$. CSR is the ratio of the average cyclic shear stress (τ) developed on horizontal surfaces as a result of the cyclic loading to generate an increment of pore water pressure equal to the initial mean effective stress (p'_0) acting on the soil layer (Seed *et al.* 1983).

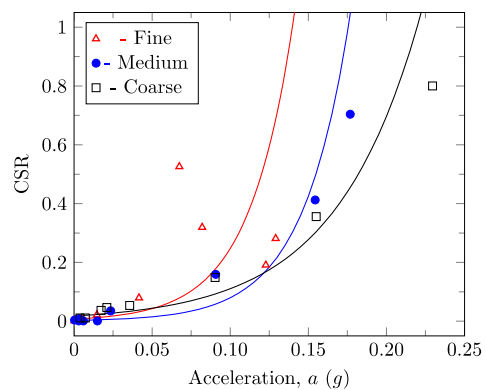
Been and Jefferies (1985) have proved, in a pioneering work, that the liquefaction resistance is associated with the critical state of the soil. Such association involves the state parameter (ψ), which is the difference of the initial void ratio with the void ratio at the critical state condition. Soils with positive values of ψ have contractile behaviour and are more susceptible to liquefaction phenomena. However, Jefferies and Been (2015) mentioned that dilative soils with moderate negative values of ψ are susceptible to liquefaction. Table 7 showed that tests in the three grain size distributions of Guamo Sand at higher frequencies are more

Table 6 Physical modelling results

Test input		Fine sandy soil			Medium sandy soil			Coarse sandy soil		
A (mV)	F (Hz)	Dr (%)	ψ	Trigger	Dr (%)	ψ	Trigger	Dr (%)	ψ	Trigger
200	1.34	24	-0.08	Non	24	-0.08	Non	24	-0.08	Non
	1.45	24	-0.08	Non	24	-0.08	Non	26	-0.09	Non
	2.04	26	-0.08	Non	23	-0.08	Non	23	-0.07	Non
500	1.34	26	-0.09	Non	19	-0.07	Non	20	-0.07	Non
	1.45	22	-0.07	Non	26	-0.08	Non	23	-0.07	Non
	2.04	22	-0.08	Non	24	-0.08	Non	26	-0.08	Non
800	1.34	20	-0.08	Non	22	-0.07	Non	27	-0.08	Non
	1.45	22	-0.08	Non	26	-0.08	Non	24	-0.08	Non
	2.04	23	-0.08	Non	28	-0.09	Non	22	-0.07	Non
200	90	23	-0.08	Non	17	-0.07	Non	22	-0.07	Non
	105	26	-0.08	Non	23	-0.08	Non	24	-0.08	Non
	208	17	-0.07	Non	23	-0.08	Non	20	-0.07	Non
500	90	27	-0.08	Non	24	-0.08	Non	24	-0.08	Non
	105	21	-0.07	Non	22	-0.07	Non	21	-0.07	Non
	208	23	-0.07	Non	20	-0.07	Non	23	-0.07	Non
800	90	24	-0.08	Liquefaction	23	-0.08	Non	22	-0.08	Non
	105	23	-0.08	Liquefaction	25	-0.08	Liquefaction	21	-0.07	Non
	208	25	-0.08	Liquefaction	27	-0.09	Liquefaction	21	-0.07	Liquefaction
200	144	22	-0.07	Liquefaction	23	-0.07	Liquefaction	22	-0.07	Liquefaction
	168	25	-0.08	Liquefaction	22	-0.07	Liquefaction	25	-0.08	Liquefaction
	332	19	-0.07	Liquefaction	21	-0.07	Liquefaction	21	-0.07	Liquefaction
500	144	21	-0.07	Liquefaction	25	-0.08	Liquefaction	26	-0.09	Liquefaction
	168	23	-0.08	Liquefaction	27	-0.08	Liquefaction	19	-0.06	Liquefaction
	332	22	-0.08	Liquefaction	20	-0.08	Liquefaction	25	-0.08	Liquefaction
800	144	22	-0.07	Liquefaction	24	-0.07	Liquefaction	20	-0.07	Liquefaction
	168	24	-0.08	Liquefaction	20	-0.07	Liquefaction	23	-0.07	Liquefaction
	332	23	-0.08	Liquefaction	22	-0.07	Liquefaction	25	-0.08	Liquefaction



(a) Resistance as a function of the number of cycles



(b) Resistance as a function of the acceleration

Fig. 12 Liquefaction susceptibility curves for Guamo Sand

susceptible to trigger the liquefaction than the tests performed at lower frequencies.

Fig. 12 presents the resistance curves of the soils in terms of the number of cycles and the acceleration applied

at the base of the micro shaking table. Such Figure indicates an effect in liquefaction susceptibility according to the particle size of the Guamo Sand. The fine soil has less resistance than the medium soil and, likewise, the medium

soil has less resistance than the coarse soil. The grain size distribution is a key factor in the accumulation of pore water pressure in granular soils due to its permeability and drainage capacity during the cyclic loading (Ishibashi 1985, Carrera *et al.* 2011).

On the other hand, it was found that the induced shear stress in the system is a product of the combination between the frequency and amplitude applied by the Piezo-Electric actuator. In the micro shaking table models, such combination controls the acceleration in the system. Hence, the acceleration applied at the base of the system is the factor for triggering the soil liquefaction phenomena during the test, as described by El-sekelly *et al.* (2015). Tsaparli *et al.* (2017) presented experimental evidence for proving that the ground motion acceleration controls the energy of physical models in shaking table devices, which in this research was applied at the container base. In addition, it was found that during the low-frequency tests the material managed to dissipate the pore water pressure excess at the surface because the low acceleration induced in the system was not warranting an undrained cyclic condition, as it is described by El-sekelly *et al.* (2015).

Based on the experimental results, the Eqs (7)-(12) were derived. Eqs. (7)-(9) present the liquefaction resistance curves as a function of the number of cycles, while Eqs. (10)-(12) present the liquefaction resistance as a function of the system acceleration. The equations that relate the CSR as a function of the number of cycles presented the traditional potential fitting obtained by Viana da Fonseca *et al.* (2015). Moreover, the equations that relate the CSR as a function of a showed an exponential fitting, which offers an acceptable fit to describe the soil liquefaction resistance according to the results obtained by El-sekelly *et al.* (2015).

$$CSR_F = 7.3179N^{-1.8290} \quad (7)$$

$$CSR_M = 77.1846N^{-2.022} \quad (8)$$

$$CSR_C = 50.1667N^{-2.094} \quad (9)$$

$$CSR_F = 0.0074exp^{35.09a} \quad (10)$$

$$CSR_M = 0.0028exp^{33.48a} \quad (11)$$

$$CSR_C = 0.0175exp^{18.21a} \quad (12)$$

6. Conclusions

This paper addresses the construction of a flexible, impermeable and frictionless container, as well as the instrumentation of a micro shaking table device to evaluate the dynamic behaviour of soils. This device allowed assessing the soil liquefaction by the application of dynamic loads with different amplitudes and frequencies. Samples prepared from three different and parallel grain size distributions of Guamo Sand were prepared. Therefore, it was performed an experimental plan of 81 physical modelling tests, which validated the state condition and the dynamic load as the factors to replicate the phenomena in the apparatus. The following conclusions can be drawn:

- The micro shaking table is able to replicate earthquakes by the appropriate combination of amplitude and frequency in a sinusoidal signal. The system response is evaluated by displacements and accelerations measurements. Therefore, it was found that the voltage amplitude defines the displacement and the signal frequency controls acceleration in the device.

- The water deposition allowed obtaining specimens of sand with a uniform initial void ratio. The above was demonstrated by the median values of Dr in all materials, which corresponded to 22.94%, 23.44% and 23.62% for fine, medium and coarse grain size distribution, respectively. In addition, this method of preparation ensures the soil saturation, due to the particle accommodation inside of the water during the sedimentation process.

- The triggering of liquefaction was estimated by the comparison between pore water pressure build-up measurement and acceleration data. Besides, the liquefaction phenomena were observed through the soil densification and water rise in the physical model. In accordance, the liquefaction triggering was identified by $r_u > 0.90$ and the soil stiffness reduction.

- The system acceleration is the key factor to induce the pore water pressure build-up of physical models in shaking tables devices. In addition, the frequency of the input signal controls the liquefaction triggering since the frequency establishes the system acceleration. Therefore, high accelerations generate high shear stresses in the soil and are more appropriate to trigger the soil liquefaction.

Acknowledgments

The authors acknowledge the Portuguese Foundation for Science and Technology (FCT) for the support of the PTDC/ECM/GEO/1780/2014 project "Liquefaction Assessment Protocols to Protect Critical Infrastructures against Earthquake Damage: LIQ2PROEARTH".

References

- Alarcón-Guzmán, A., Leonards, G.A. and Chameau, J.L. (1988), "Undrained monotonic and cyclic strength of sands", *J. Geotech. Eng.*, **114**(10), 1089-1109. [https://doi.org/10.1061/\(ASCE\)0733-9410\(1988\)114:10\(1089\)](https://doi.org/10.1061/(ASCE)0733-9410(1988)114:10(1089)).
- ASTM International (2007), *D422 - Standard Test Method for Particle-Size Analysis of Soils*.
- ASTM International (2014), *D854 - Standard Test Methods for Specific Gravity of Soil Solids by Water Pycnometer*.
- ASTM International (2016), *D4254 - Standard Test Methods for Minimum Index Density and Unit Weight of Soils and Calculation of Relative Density*.
- Been, K. and Jefferies, M. (1985), "A state parameter for sands", *Geotechnique*, **35**(2), 99-112.
- Bertalot, D. and Brennan, A.J. (2015), "Influence of initial stress distribution on liquefaction-induced settlement of shallow foundations", *Geotechnique*, **65**(5), 418-428. <http://dx.doi.org/10.1680/geot.SIP.15.P.002>.
- Caicedo, B., Tristancho, J. and Thorel, L. (2015), "Mathematical and physical modelling of rainfall in centrifuge", *Int. J. Phys. Modell. Geotech.*, **15**(3), 150-164. <http://dx.doi.org/10.1680/ijpmsg.14.00023>.

- Carrera, A., Coop, M. and Lancellota, R. (2011), "Influence of grading on the mechanical behaviour of Stava tailings", *Géotechnique*, **61**(11), 935-946. <http://dx.doi.org/10.1680/geot.9.P.009>.
- Cho, G., Dodds, J. and Santamarina, J.C., (2006), "Particle shape effects on packing density, stiffness, and strength: natural and crushed sand", *J. Geotech. Geoenviron. Eng.*, **132**(5), 591-602. [https://doi.org/10.1061/\(ASCE\)1090-0241\(2006\)132:5\(591\)](https://doi.org/10.1061/(ASCE)1090-0241(2006)132:5(591)).
- Coelho, P.A.L.F, Haigh, S.K. and Madabhushi, S.P.G. (2006), "Effects of successive earthquakes on saturated deposits of sand", *Proceedings of the Sixth International Conference on Physical Modelling in Geotechnics-6th ICPMG '06*, Hong Kong, August.
- Correa, W. (2015), "Shaking box design, construction and test on small shaking table and centrifuge modeling", Ph.D. Dissertation, Universidad de los Andes, Bogota, Colombia.
- Dashti, S., Bray, J.D., Pestana, J.M., Riemer, M. and Wilson, D. (2006), "Mechanisms of seismically induced settlement of buildings with shallow foundations on liquefiable soil", *J. Geotech. Geoenviron. Eng.*, **136**(1), 151-164. [https://doi.org/10.1061/\(ASCE\)GT.1943-5606.0000179](https://doi.org/10.1061/(ASCE)GT.1943-5606.0000179).
- Du, S. and Chian, S.C. (2018), "Excess pore pressure generation in sand under non-uniform cyclic strain triaxial testing", *Soil Dyn. Earthq. Eng.*, **109**, 119-131. <https://doi.org/10.1016/j.soildyn.2018.03.016>.
- El-sekelly, W., Dobry, R., Abdoun, T. and Steidl, J.H. (2015), "Centrifuge modeling of the effect of preshaking on the liquefaction resistance of silty sand deposits", *J. Geotech. Geoenviron. Eng.*, **142**(6), 1211-1226. [https://doi.org/10.1061/\(ASCE\)GT.1943-5606.0001430](https://doi.org/10.1061/(ASCE)GT.1943-5606.0001430).
- Georgiannou, V.N., Tsomokos, A. and Stavrou, K. (2008), "Monotonic and cyclic behaviour of sand under torsional loading", *Géotechnique*, **58**(2), 113-124. <https://doi.org/10.1680/geot.2008.58.2.113>.
- Green, R.A., Cubrinovski, M., Bradley, B., Henderson, D., Kailey, P., Robinson, K., Taylor, M., Winkley, A., Wotherspoon, L., Oresne, R., Pender, M., Hogan, L., Allen, J., Bradshaw, A., Bray, J., DePascale, G., O'Rourke, T., Rix, G., Wells, D. and Wood, C. (2012), "Geotechnical aspects of the Mw 6.2 2011 Christchurch, New Zealand, Earthquake", *Proceedings of the GeoCongress 2012: State of the Art and Practice in Geotechnical Engineering*, Oakland, California, U.S.A.
- Hushmand, B., Scott, R.F. and Crouse, C.B. (1988), "Centrifuge liquefaction tests in a laminar box", *Géotechnique*, **38**(2), 253-262.
- Iai, S. (1988), "Similitude for shaking table tests on soil-structure-fluid model in 1g gravitational field", *Soils Found.*, **29**(1), 105-118. <https://doi.org/10.3208/sandfl.1972.29.105>.
- Idriss, I.M. and Boulanger, R.W. (2012), *Soil Liquefaction during Earthquakes*, Earthquake Engineering Research Institute, Oakland, California, U.S.A.
- INVIAS (2013), "INV E-136-13 Estimation of the unit weight maximum and minimum for the computation of relative density".
- Ishibashi, I. (1985), "Effect of grain characteristics on liquefaction potential-In search of standard sand for cyclic strength", *Geotech. Test. J.*, **8**(3), 137-139. <https://doi.org/10.1520/GTJ10525J>.
- Ishihara, K. (1996), *Geotechnical Earthquake Engineering*, Prentice Hall, New York, U.S.A.
- Ishihara, K. (1996), *Soil Behaviour in Earthquake Geotechnics*, Oxford, New York, U.S.A.
- Jefferies, M. and Been, K. (2015), *Soil Liquefaction: A Critical State Approach*, CRC Press, Abingdon, U.K.
- Jiménez, O. and Lizcano, A. (2015), "Liquefaction flow behavior of Guamo sand", *Proceedings of the 15th Pan American Conference on Soil Mechanics and Geotechnical Engineering*, Buenos Aires, Argentina, November.
- Kramer, S. and Elgamal, A.M. (2001), *Modeling Soil Liquefaction Hazards for Performance-based Earthquake Engineering*, Pacific Earthquake Engineering Research Center, Berkeley, California, U.S.A.
- Lin, M. and Wang, K. (2006), "Seismic slope behavior in a large-scale shaking table model test", *Eng. Geol.*, **86**(2-3), 118-133. <https://doi.org/10.1016/j.enggeo.2006.02.011>.
- Madabhushi, G. (2014), *Centrifuge Modelling for Civil Engineers*, CRC Press, New York, U.S.A.
- Madabhushi, S.P.G. and Schofield, A.N. (1993), "Centrifuge modelling of tower structures on saturated sands subjected to earthquake perturbations", *Géotechnique*, **43**(4), 555-565. <https://doi.org/10.1680/geot.1993.43.4.555>.
- Meymand, P. (1998), "Shaking table scale model tests of nonlinear soil-pile-superstructure interaction in soft clay", Ph.D. Dissertation, University of California, Berkeley, California, U.S.A.
- Moczo, P., Kristek, J. and Gális, M. (2014), *The Finite-Difference Modelling of Earthquake Motions: Waves and Ruptures*, Cambridge University Press, Cambridge, U.K.
- Monkul, M.M., Gültekin, C., Güvler, M., Akın, Ö. and Eseller-Bayat, E. (2015), "Cyclic DSS tests for the evaluation of stress densification effects in liquefaction assessment", *Soil Dyn. Earthq. Eng.*, **75**, 27-36. <https://doi.org/10.1016/j.soildyn.2015.03.016>.
- Patiño, J. (2015), "Hipoplastic parameters of Guamo Sand", M.Sc. Dissertation, Universidad de Los Andes, Bogota, Colombia.
- Ramos, C., Viana da Fonseca, A. and Vaunat, J. (2015), "Modeling flow instability of an Algerian sand with the dilatancy rule in CASM", *Geomech. Eng.*, **9**(6), 729-742. <http://dx.doi.org/10.12989/gae.2015.9.6.729>.
- Robertson, P.K. (2010), "Evaluation of flow liquefaction and liquefied strength using the cone penetration test", *J. Geotech. Geoenviron. Eng.*, **136**(6), 842-853. [https://doi.org/10.1061/\(ASCE\)GT.1943-5606.0000286](https://doi.org/10.1061/(ASCE)GT.1943-5606.0000286).
- Robertson, P.K. and Wride, C.E. (1998), "Evaluating cyclic liquefaction potential using the cone penetration test", *Can. Geotech. J.*, **35**(3), 442-459. <https://doi.org/10.1139/t98-017>.
- Sarmiento, C.A. and Vidal, H.A. (2007), "Geomechanical characterization of soil mixtures for physical models by the method of equivalent materials", B.Sc. dissertation, Universidad de la Salle, Bogota, Colombia (in Spanish).
- Seed, H.B. and Idriss, I.M. (1971), "Simplified procedure for evaluating soil liquefaction potential", *J. Soil Mech. Found.*, **97**(9), 1249-1273.
- Seed, H.B., Idriss, I.M. and Arango, I. (1983), "Evaluation of liquefaction potential using field performance data", *J. Geotech. Eng.*, **109**(3), 458-482. [https://doi.org/10.1061/\(ASCE\)0733-9410\(1983\)109:3\(458\)](https://doi.org/10.1061/(ASCE)0733-9410(1983)109:3(458)).
- Serrato, D.P. (2012), "Design of a flexible soil-container used on small shaking tables and centrifuge models", B.Sc. Dissertation, Universidad de Los Andes, Bogota, Colombia.
- Sharp, M., Dobry, R. and Phillips, R. (2010), "CPT-Based evaluation of liquefaction and lateral spreading in centrifuge", *J. Geotech. Geoenviron. Eng.*, **136**(10), 1334-1346. [https://doi.org/10.1061/\(ASCE\)GT.1943-5606.0000338](https://doi.org/10.1061/(ASCE)GT.1943-5606.0000338).
- Taylor, R. (1995), *Geotechnical Centrifuge Technology*, Blackie Academic & Professional, London, U.K.
- Tique, D. (2016), "Experimental study of the diffuse instability for the Guamo Sand", M.Sc. Dissertation, Pontificia Universidad Javeriana, Bogota, Colombia (in Spanish).
- Tsaparli, V., Kontoe, S. and Taborda, D. (2017), "An energy-based interpretation of sand liquefaction due to vertical ground motion", *Comput. Geotech.*, **90**, 1-13. <https://doi.org/10.1016/j.compgeo.2017.05.006>.
- Turan, A., Hinchberger, S.D. and El Naggar, H. (2009), "Design

- and commissioning of a laminar soil container for use on small shaking tables”, *Soil Dyn. Earthq. Eng.*, **29**(2), 404-414. <https://doi.org/10.1016/j.soildyn.2008.04.003>.
- Ueng, T.S., Wu, C.W., Cheng, H.W. and Chen, C.H. (2010), “Settlements of saturated clean sand deposits in shaking table tests”, *Soil Dyn. Earthq. Eng.*, **30**(2), 50-60. <https://doi.org/10.1016/j.soildyn.2009.09.006>.
- Viana da Fonseca, A., Soares, M. and Fourie, A.B. (2015), “Cyclic DSS tests for the evaluation of stress densification effects in liquefaction assessment”, *Soil Dyn. Earthq. Eng.*, **75**, 98-111. <https://doi.org/10.1016/j.soildyn.2015.03.016>.
- Wang, B., Zen, K., Chen, G.Q. and Kasama, K. (2011), “Effects of excess pore pressure dissipation on liquefaction-induced ground deformation in 1-g shaking table test”, *Geomech. Eng.*, **4**(2), 91-103. <https://doi.org/10.12989/gae.2012.4.2.091>
- Zhou, J. Jiang, J. and Chen, X. (2015), “Micro- and macro-observations of liquefaction of saturated sand around buried structures in centrifuge shaking table tests”, *Soil Dyn. Earthq. Eng.*, **72**, 1-11. <https://doi.org/10.1016/j.soildyn.2014.12.017>.